Peptide Inhibition of ENaC†

Iskander I. Ismailov,‡ Vadim Gh. Shlyonsky,‡ Engin H. Serpersu,§ Catherine M. Fuller,‡ Herbert C. Cheung,‖ Donald Muccio,⊥ Bakhrom K. Berdiev,‡ and Dale J. Benos*,‡

Department of Physiology and Biophysics, Department of Chemistry, Department of Biochemistry and Molecular Genetics, University of Alabama at Birmingham, Birmingham, Alabama 35294-0005, and Department of Biochemistry and Cellular and Molecular Biology, University of Tennessee, Knoxville, Tennessee 37996-0840

Received August 17, 1998; Revised Manuscript Received October 16, 1998

ABSTRACT: Liddle's disease is an autosomal dominant form of human hypertension resulting from a basal activation of amiloride-sensitive Na^+ channels (ENaC). This channel activation is produced by mutations in the β- and/or γ-carboxy-terminal cytoplasmic tails, in many cases causing a truncation of the last 45−76 amino acids. In this study, we tested two hypotheses; first, β- and γ-ENaC C-terminal truncation mutants ($\beta_{\Delta C}$ and $\gamma_{\Delta C}$), in combination with the wild-type α-ENaC subunit, reproduce the Liddle's phenotype at the single channel level, i.e., an increase in open probability (P_o), and second, these C-terminal regions of β- and γ-ENaC act as intrinsic blockers of this channel. Our results indicate that $\alpha\beta_{\Delta C}\gamma_{\Delta C}$-rENaC, incorporated into planar lipid bilayers, has a significantly higher single channel P_o compared to the wild-type channel (0.85 vs 0.60, respectively), and that 30-mer synthetic peptides corresponding to the C-terminal region of either β- or γ-ENaC block the basal-activated channel in a concentration-dependent fashion. Moreover, there was a synergy between the peptides for channel inhibition when added together. We conclude that the increase in macroscopic Na^+ reabsorption that occurs in Liddle's disease is at least in part due to an increase in single channel P_o and that the cytoplasmic tails of the β- and γ-ENaC subunits are important in the modulation of ENaC activity.

Despite intensive investigation, the primary determinants of hypertension remain unknown in the overwhelming majority of affected individuals. The identification of the cause of hypertension in any given individual is confounded by the multifactorial nature of this disease. However, it has been estimated that anywhere from 20 to 60% of the population variability in blood pressure is genetically determined (*1*−*3*). Liddle's syndrome is a form of autosomal dominant, low renin, volume expanded, salt-sensitive hypertension. The basic clinical features of this syndrome (pseudohyperaldosteronism) were first described in an Alabama family in 1963 (*4*). The original patient developed renal failure in 1989 and underwent successful renal transplantation (*5*). The subsequent resolution of the patient's hypertension supported Liddle's original contention that this disorder resulted from a greatly enhanced ability of the kidneys to reabsorb salt. Further support for this idea came from clinical observations that the hypokalemia and hypertension associated with Liddle's syndrome could be alleviated with triamterine or amiloride therapy (*6*). Genetic linkage studies identified the causal mutation of this hypertensive disease to exist in the β subunit of the recently cloned amiloride-sensitive Na^+ channel, ENaC (*7*). Subsequently, mutations in the γ subunit of this channel have also been noted (*8*); these mutations also produce basal activation of these channels, and indicate heterogeneity of this disease (see refs *9*−*11* for discussion).

All of the aforementioned mutations introduced premature stop codons or frame-shift mutations in the segments encoding the cytoplasmically located C-termini of either β- or γ-ENaC, effectively eliminating the terminal 45−76 amino acids. Expression of truncated β- or γ-ENaC subunits in *Xenopus* oocytes with normal α-ENaC produced a markedly enhanced amiloride-sensitive sodium current as compared to oocytes injected with wild-type (WT) α-, β-, γ-rENaC (*12*−*14*). Two mechanisms have been suggested that could account for the increased macroscopic current: elevated surface expression of channels (*13*, *15*−*17*), and a defect in the channel gating mechanism such that the channel stays open most of the time (*18*, *19*). Recent studies using ^{125}I-labeled M2 anti-FLAG antibody binding (*19*) or immunofluorescence (*20*) in ENaC-expressing oocytes revealed that one mutation akin to that found in Liddle's disease, namely, β-rENaC subunit R564X, produced a small increase in channel surface expression, but not enough to account for the increased macroscopic currents.

Using planar lipid bilayers, we have tested the hypothesis that the single channel characteristics of α-, β-, and γ-ENaC could be modified to reproduce the Liddle's phenotype, i.e., enhanced Na^+ channel activity. We also aimed to elucidate the nature of the regulation that the β- and γ-ENaC C-termini subunits confer upon amiloride-sensitive Na^+ channels, testing the hypothesis that the terminal cytoplasmic carboxy tails of β- and γ-ENaC act in association as a channel inactivation peptide. Our results indicate that removal of the β- and/or γ-ENaC carboxy tails result in an increased single

† This work was supported by NIH Grant DK37206.
* To whom correspondence should be addressed.
‡ Department of Physiology and Biophysics.
§ University of Tennessee.
‖ Department of Biochemistry and Molecular Genetics.
⊥ Department of Chemistry.

10.1021/bi981979s CCC: $18.00
Published on Web 12/09/1998

channel open probability and that 30-mer peptides constructed from the C-terminal tails of either of these subunits can effectively reduce single channel open probability by "locking" the channel in its closed state. Importantly, there appears to be a synergy between the actions of the β- and γ- peptides: when present in solution together, the inhibition was greater than that produced by the individual peptides themselves. Therefore, we conclude that the terminal cytoplasmic carboxy tail of the β- and γ-ENaC subunits act in concert as an inactivation peptide by binding to an internal region of the Na^+ channel and closing the channel. However, the inhibition of the channel by these peptides is distinctly different than the "ball and chain" model originally proposed for blockade of *Shaker* K^+ channels (*21*, *22*), in that the peptides are not acting as open channel blockers.

MATERIALS AND METHODS

Circular Dichroism Spectroscopy. Far-UV circular dichroism (CD) spectra of peptides were recorded on an AVIV 62DS spectropolarimeter at 25 °C. Data points were taken every 0.5 nm using a 1 s averaging time and 1.5 nm bandwidth. Peptide concentrations were 500 μM in 30 mM K_2HPO_4 buffer, pH 7.0. Ten scans were averaged for sample and buffer spectra, which were obtained with identical parameters. The peptide spectra were obtained by baseline subtracting the buffer spectrum, and then the spectrum was converted to mean residue ellipticity in deg cm^2 $dmol^{-1}$ (*23*). Secondary structure calculations were performed using PROSEC (AVIV Instruments; Lakewood, NJ) based on the method of Yang and co-workers (*24*).

Steady-State Fluorescence Measurements. Solution fluorescence measurements were made on a PTI M-series spectrophotometer at 20 °C in a buffer containing 0.1 mM NaCl and 10 mM Tris-HCl (pH 7.4). The excitation wavelength was 275 nm with a 2 nm band-pass. The band-pass for emission was 3 nm. Quantum yields of tyrosine in peptides were determined by a comparative method, using L-tyrosine as a standard with its quantum yield assumed to be 0.21 (*25*). Quantum yields (q) were calculated according to the formula

$$q = q_{st}[I(1 - T_{st})]/[I_{st}(1 - T)]$$

where q_{st} is quantum yield of L-tyrosine, and $T = 10^{-A}$, where A is absorbance at the wavelength of excitation. Spectral absorbance was measured using a Beckman DU-40 spectrophotometer. The absorbances were corrected for light scattering by extrapolation of the scattering/wavelength plot (*26*, *27*). Where necessary, corrections for inner filter effects were also made.

Peptide Synthesis. All peptides were synthesized by Research Genetics (Huntsville, AL). They were purified by reversed-phase, high-performance liquid chromatography to a purity of >90%. All purified peptides were analyzed for amino acid composition by mass spectroscopy. The primary amino acid sequences of the peptides used in this study were $SP_{30}\beta$, ^{611}PIPGTPPPNYDSLRLQPLDVIESDSEGDAI^{640}; $SP_{30}\gamma$, ^{620}PGTPPPKYNTLRLERAFSNQLTDTQMLDEL^{649}; Pro-$SP_{30}\beta$, ^{611}P**P**PGTPPPNYDSLRLQPLD**PP**ESDSEGDAD^{640}; and Asp-$SP_{30}\beta$, ^{611}P**D**PGTPPPNYDSLRLQPLD**DD**ESDSEGDAD^{640}.

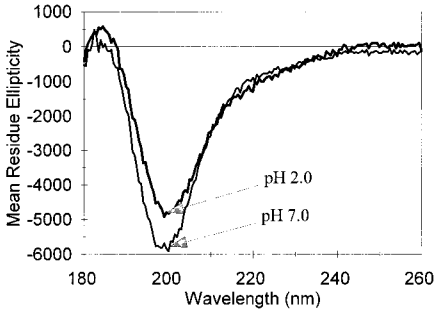

FIGURE 1: Far-UV CD spectra of $SP_{30}\beta$. $SP_{30}\beta$ peptide (500 μM) was dissolved in 30 mM K_2HPO_4 buffer, pH 2.0 and pH 7.0. The spectra were measured at 25 °C in a 0.1 mm cell. The CD spectrum of $SP_{30}\gamma$ was very similar.

Planar Lipid Bilayers. The methodology used in the planar lipid bilayer experiments has been described in detail previously (*18*, *28*). In brief, bilayer membranes were made from a mixture of 2:1 (wt/wt) diphytanoylphosphatidylethanolamine:diphytanoylphosphatidylserine in octane (final concentration 25 mg/mL). The membranes were painted with a glass rod over a 200 μm hole drilled in a polystyrene cup. The standard solution that bathed both sides of the membranes was 100 mM NaCl, 10 mM 3-(*N*-morpholino)-propanesulfonic acid (MOPS), pH 7.4. All potentials are referred to the trans chamber, which was connected to the input stage of the current−voltage converter. Data analysis was performed as previously described (*29*−*31*). In vitro transcription of individual α-, β-, or γ-rENaC subunits was performed as previously described (*29*−*31*). All ENaC cDNA constructs were kind gifts of Drs. Cecilia Canessa (Yale University) and Bernard Rossier (Universität de Lausanne). Proteoliposomes containing the transcribed subunits were made as described (*29*−*31*). Liposomes were subsequently fused to the lipid bilayer for recording single channel current. In most of the experiments reported in this paper, liposomes were pretreated with 25 μM DTT for 2 min, washed, and then subjected to two freeze−thaw cycles followed by a brief (30 s) period of sonication. Under these circumstances, a single conduction unit was observed, thus simplifying the data analysis procedure (see Refs *29* and *31* and below for discussion of ENaC single channel kinetics). The experiments were also performed on non-DTT-treated vesicles with essentially comparable outcomes.

RESULTS

Interaction between C-Terminal Peptides in Solution. As a prelude to testing the hypothesis that the C-terminal domains of β- and γ-ENaC interact with each other, circular dichroism (CD) spectroscopic studies were performed to determine if β- and γ-ENaC C-terminal peptides adopt a defined structure in aqueous solution. The CD spectra of the 30-mer β-hENaC peptide (30 mM KH_2PO_4) at pH 2.0 and 7.0 are displayed in Figure 1. Comparable spectra were measured for the $SP_{30}\gamma$ peptide (not shown). These spectra lack a strong negative band centered between 190 and 200 nm that is characteristic of peptides and proteins in the unfolded state (*23*). Instead, the spectra displayed a weak minimum at 200 nm and positive band centered at 185 nm (pH 2.0). Using proteins as a basis for evaluation, the intensity of the negative band is more consistent with CD spectra associated with all-β sheet proteins (*23*, *32*). How-

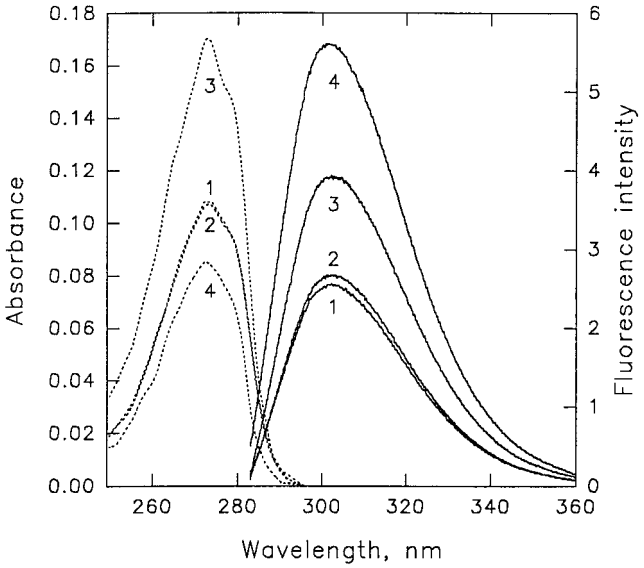

FIGURE 2: Absorbance and tyrosine fluorescence spectra of peptides comprising C-termini of β and γ subunits individually and in a 1:1 $\beta + \gamma$ peptide mixture. Absorbance spectra corrected for light scattering (dashed lines) and fluorescence spectra (solid lines) of (1) 100 μM $SP_{30}\beta$; (2) 100 μM $SP_{30}\gamma$; (3) 50 μM $SP_{30}\beta$ + 50 μM $SP_{30}\gamma$; and (4) 100 μM L-tyrosine. All spectra were measured in 0.1 mM NaCl, 10 mM Tris-HCl (pH 7.4) and were repeated a minimum of 3 times.

ever, there are some examples of all-β proteins (e.g., elastase) that display negative bands near 200 nm, which make deciding between unfolded proteins and all-β proteins difficult (*33*). The secondary structure content estimate of the 30-mer β-hENaC peptide was 65% β-sheet structure, 30% unordered, and 5% helical turns using the methodology of Chang et al. (*24*). When the peptide was placed at pH 7.0, a small decrease in the 185 nm band and increase in negative amplitude of the 200 nm band occurred. This is consistent with slightly less β-sheet structure (about a 5% decrease) and slightly more unordered structure.

If both $SP_{30}\beta$ and $SP_{30}\gamma$ in solution adopt a β-sheet structure, it is plausible to hypothesize that the two β-sheet structures can interact with each other. This idea was tested directly in a series of absorption and fluorescence experiments in which the spectral properties of individual $SP_{30}\beta$ and $SP_{30}\gamma$ peptides were compared with those from a mixture of the peptides (Figure 2). The absorption spectra of the single tyrosine in both peptides (Tyr 620 in $SP_{30}\beta$ and Tyr 627 in $SP_{30}\gamma$) were indistinguishable from each other (curves 1 and 2, left panel). An equivalent mixture of the two peptides showed an increase of over 50% in the peak absorbance (curve 3). Because the tyrosine absorption band is an $n \rightarrow \pi^*$ transition, the increased absorbance observed with the mixture suggests that the tyrosine in one or both peptides experienced a less polar environment. Such an environmental change supports the idea of an interaction between the two peptides. The fluorescence spectra (right panel) of the individual peptides and their mixture had a maximum (303 nm) similar to that of L-tyrosine. The spectrum for the mixture (curve 3) displayed a considerably higher intensity than either of the two peptides (curves 1 and 2). This apparent higher intensity was consistent with a larger absorbance of the sample at the excitation wavelength. The quantum yields of these samples are summarized in Table 1. The quantum yield for the ($\beta + \gamma$) peptide mixture

Table 1: Fluorescence Spectra of C-Terminal 30-mer β- and γ-hENaC Peptides[a]

peptide	q (quantum yield)	% decrease	number
$SP_{30}\beta$ (100 μM)	0.072 ± 0.001		4
$SP_{30}\gamma$ (100 μM)	0.074 ± 0.001		4
$SP_{30}\beta$ (50 μM) + $SP_{30}\gamma$ (50 μM)	0.065 ± 0.001	11.0	4
Pro-$SP_{30}\beta$ (100 μM)	0.071 ± 0.001		3
Pro-$SP_{30}\beta$ (50 μM) + $SP_{30}\gamma$ (50 μM)	0.067 ± 0.001	7.6	3
Asp-$SP_{30}\beta$ (100 μM)	0.065 ± 0.001		3
Asp-$SP_{30}\beta$ (50 μM) + $SP_{30}\gamma$ (50 μM)	0.067 ± 0.001	3.6	3

[a] Percent decrease in average quantum yield was calculated in comparison to the respective wild-type peptide. For the mixtures, the mean q for the appropriate individual peptides was used as the standard.

was 11% smaller than either of the peptides. This quenching of tyrosine fluorescence is additional support of an interaction between the β and γ peptide. NMR studies of the peptides alone and as a mixture suggested that they were rapidly tumbling and quite flexible in solution. The data precluded a more detailed structural analyses due to lack and/or weakness of observable dipolar interactions.

Peptide Inhibition of Basal-Activated $\alpha\beta_{\Delta C}\gamma_{\Delta C}$ ENaC in Planar Lipid Bilayers. Functional experiments were performed next to test directly the hypothesis that the C-terminal peptides could individually block basal-activated ENaC and that these peptides could interact with each other. These experiments employed an experimental design based on the finding that the concerted gating of ENaC could be disrupted by S−S bond reduction with the sulfhydryl reagent dithiothreitol (DTT) (*29*, *30*). The experimental protocol consisted of reduction of disulfide bonds with DTT prior to reconstituting the channels into proteoliposomes (*31*). When the proteoliposomes containing ENaCs were formed in the presence of 25 μM DTT using a sonication/freeze−thaw procedure, the resulting channels had perfectly uniform conductances of 13 pS and were equally sensitive to the diuretic amiloride (Figure 3A). These observations were interpreted as indicating that, following S−S bond reduction, the β- and γ-rENaC subunits did not impose an obvious modulatory action on an individual conduction element (formed by the α-ENaC subunit alone). Experiments testing this interpretation are shown in Figure 3B. Independent of DTT treatment, all channels composed of the WT α- and C-terminal truncated β- and γ-rENaC subunits (i.e., $\alpha\beta_{\Delta C}\gamma$, $\alpha\beta\gamma_{\Delta C}$, and $\alpha\beta_{\Delta C}\gamma_{\Delta C}$) displayed a significantly higher open probability ($P_o \geq 0.85$ versus $P_o = 0.63 \pm 0.07$ for the all WT channels), thus producing a basal-activated Na^+ channel. It therefore appears likely that in a 1:1:1 mixture, all α-, β-, and γ-ENaC subunits associate forming functional α-, $\alpha\beta$-, $\alpha\gamma$-, $\alpha\beta\gamma$-channels. However, because $\alpha\beta\gamma$-rENaC dominates, these results suggest a cooperative association among individual α-, β-, and γ-rENaC subunits when all three proteins are physically present. Moreover, because the constitutively activated phenotype dominated in all the experiments with C-terminally truncated β- and/or γ-ENaCs, the heterooligomeric association of α-, β-, and γ-subunits must be cooperative when at least two out of three individual subunits are present. These results support the hypothesis that the C-terminal-located, negatively charged domains of β- and γ-ENaC subunits interact with each other, thus

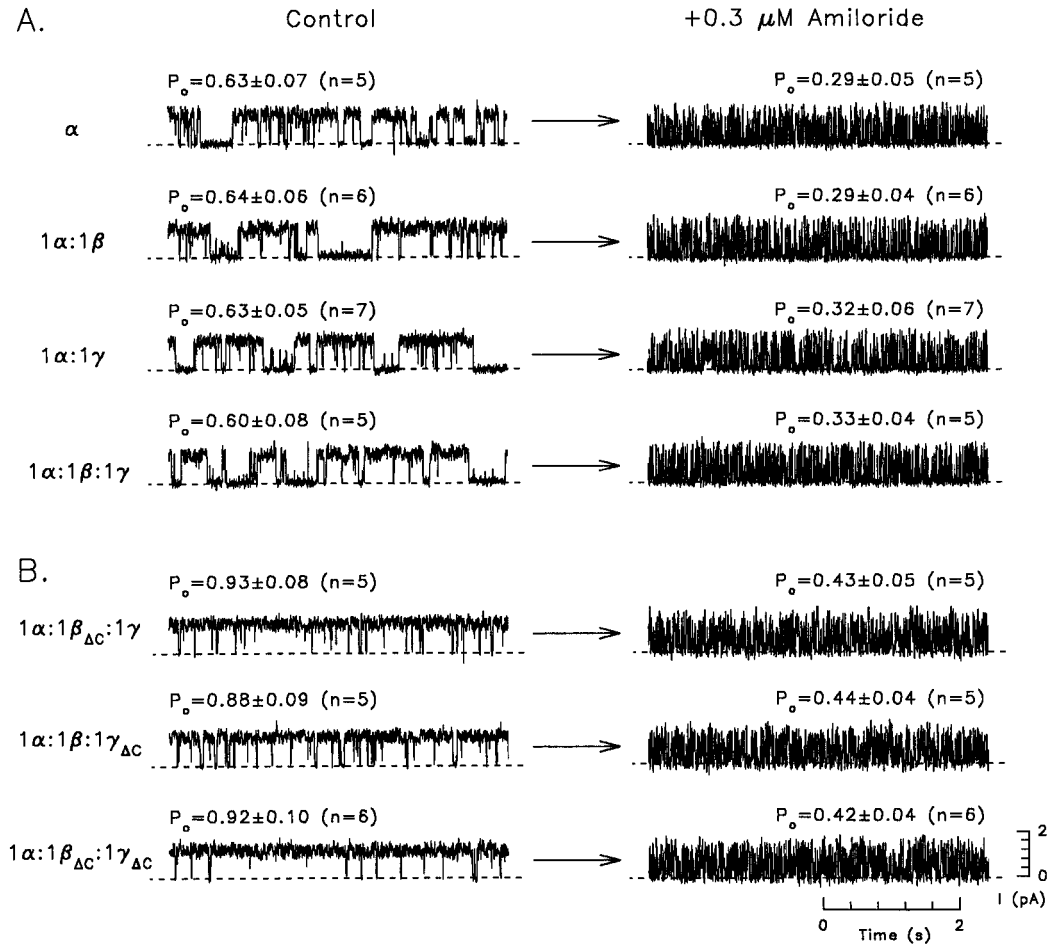

FIGURE 3: Single channel recordings and effect of amiloride on rENaC constructed of different combinations of wild-type subunits (A) and WT α-ENaC plus C-terminally truncated β and/or γ (B). In vitro translated individual ENaC subunits were reconstituted into proteolyposomes in combination, as indicated in the figure in the presence of 50 μM DTT, and incorporated into planar lipid bilayers bathed with symmetrical solutions of 100 mM NaCl and 10 mM Tris-MOPS (pH 7.4). The holding potential was +100 mV, and the dotted lines indicate zero current. The records shown were filtered at 100 Hz, and are representative of at least five separate experiments. Amiloride (0.3 μM) was added to the trans compartment to verify the identity of the channels.

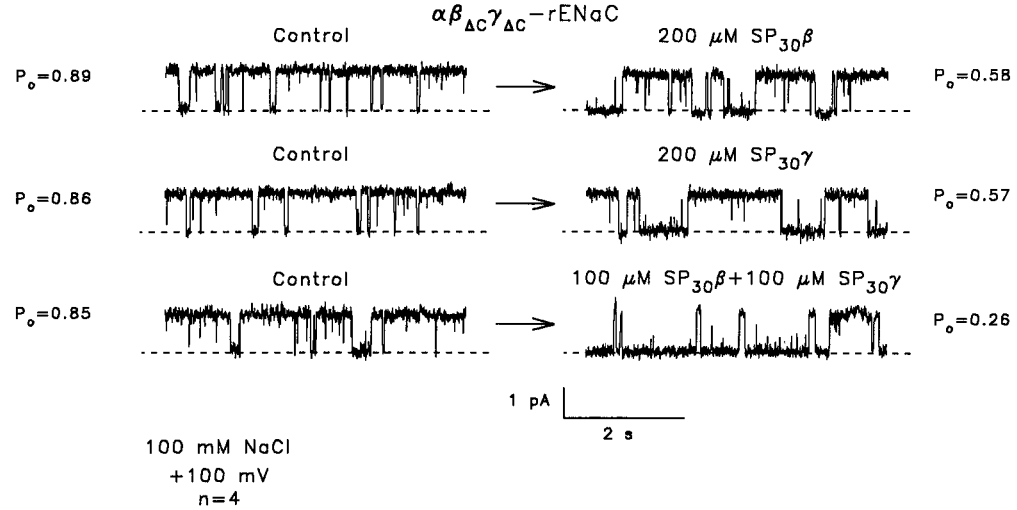

FIGURE 4: Effect of C-terminal β and/or γ peptides on $\alpha\beta_{\Delta C}\gamma_{\Delta C}$-rENaC in planar bilayers. Recording conditions and bathing solutions were the same as described in Figure 3. The 30-mer C-terminal peptides with sequences identical to the last 30 amino acids of β- or γ-rENaC were added to the cis (or presumptive "cytoplasmic") side, separately (200 μM) or together (100 μM β peptide + 100 μM γ peptide). These experiments have been repeated at least four times each with identical results.

forming an intrinsic gating mechanism within $\alpha\beta\gamma$-rENaC.

Experiments directly testing this hypothesis were based on our previous findings that a 10- or 30-amino acid carboxy-terminal peptide of β-ENaC, and a 10-amino acid C-terminal peptide of γ-ENaC, inhibit basal-activated Na^+ channels immunopurified from lymphocytes of patients affected with Liddle's disease (*18*, *34*). Either of two negatively charged 30-mer synthetic peptides comprising the C-termini of β-

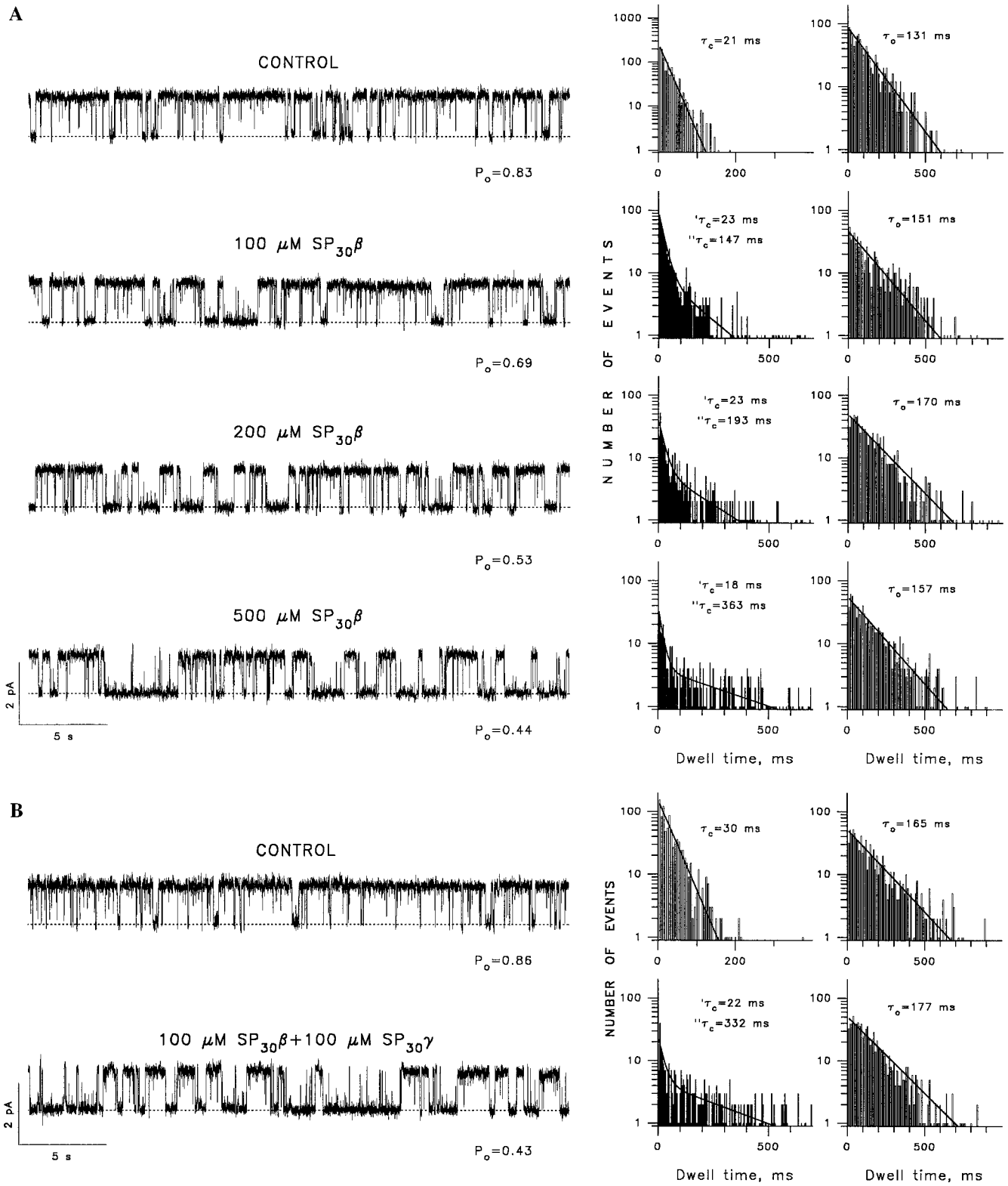

FIGURE 5: (A) Effect of increasing concentrations of SP$_{30}\beta$-terminal peptide on kinetic properties of $\alpha\beta_{\Delta C}\gamma_{\Delta C}$-rENaC in planar bilayers. Experimental conditions were identical to those indicated in the legend to Figure 3. Representative dwell time histograms were constructed from event analyses using pCLAMP software (Axon Instruments) on single channel recordings of at least 3 min duration (300 Hz filtering with an acquisition rate of 1 ms/point). Event detection thresholds were set at 50% of the current transition between open and closed states, and 3 ms in duration. The bin widths in the closed and open time histograms were 5 and 10 ms, respectively. Time constants were determined from either a single or double exponential fit of the data. Similar results have been seen for γ-SP$_{30}$ and the combination of β and γ peptides (not shown). These experiments were repeated four times for each peptide or mixture of peptides. (B) Effect of combination of SP$_{30}\beta$ and SP$_{30}\gamma$ on kinetic properties of $\alpha\beta_{\Delta C}\gamma_{\Delta C}$ r-ENaC in bilayers.

and γ-rENaC (SP$_{30}\beta$ and SP$_{30}\gamma$) decreased single channel open probability, but not the conductance, of basal-activated channels composed of wild-type α-ENaC and C-terminal truncated β and γ subunits ($\alpha\beta_{\Delta C}\gamma_{\Delta C}$-rENaC), but only when added to the cis (i.e., "cytoplasmic") bathing solution (Figure 4). Addition of 500 μM of either peptide to the trans bathing

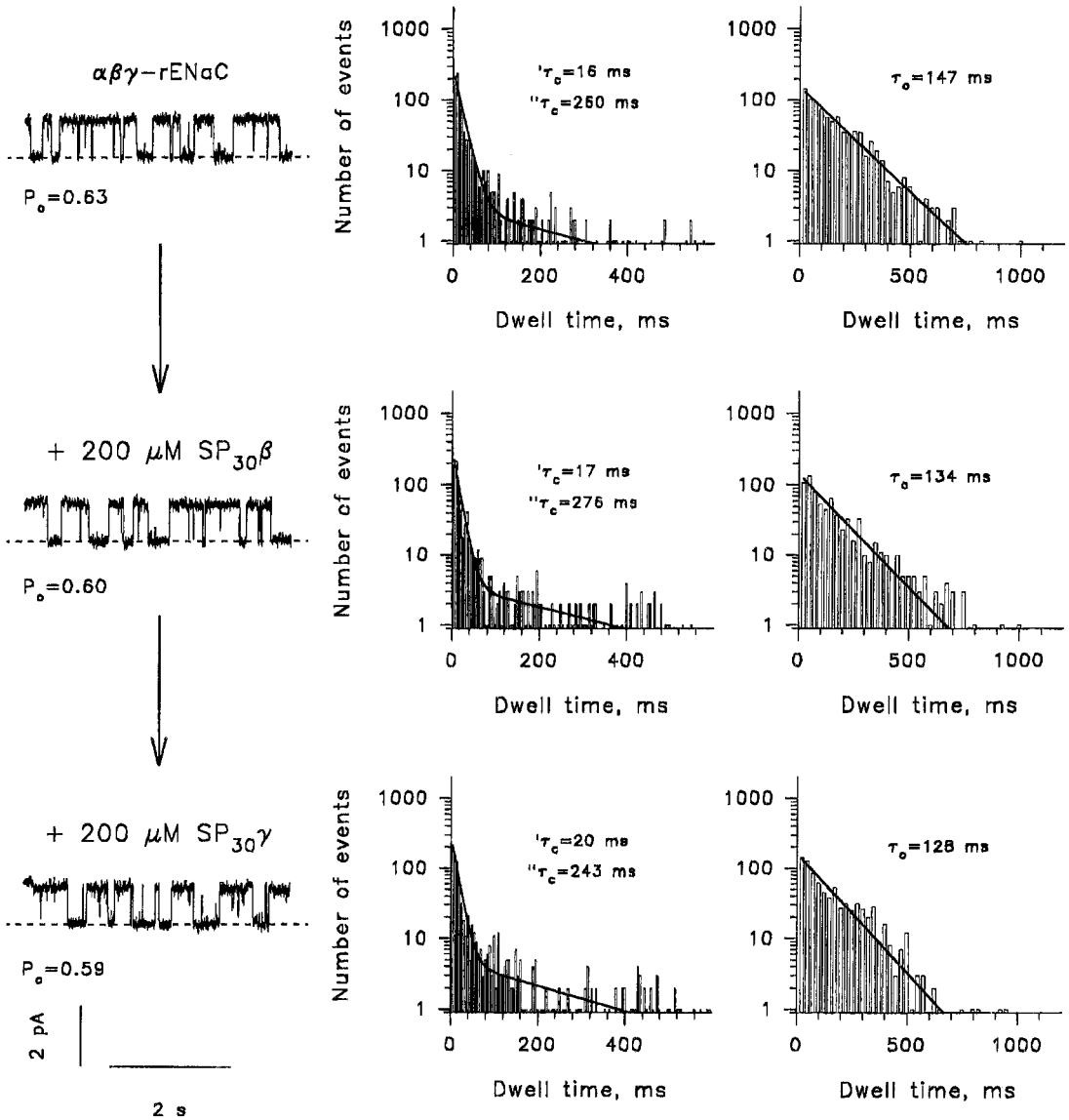

FIGURE 6: Lack of an effect of C-terminal β and γ peptides on WT $\alpha\beta\gamma$-rENaC in planar bilayers. Experimental conditions were identical to those indicated in the legend to Figure 3. Records shown are sequential and representative of at least 3 experiments with additions made as shown in the figure. Open and closed dwell time histograms are shown to the right. The bin widths in the closed and open time histograms were 5 and 25 ms, respectively. Similar results have been seen when changing the order of additions of β and γ peptides (not shown).

solution of $\alpha\beta_{\Delta C}\gamma_{\Delta C}$-rENaC-containing bilayers was without effect ($n = 4$ for each, data not shown). The individual β- and γ- peptides inhibited these channels with essentially equal efficacy (34.8 ± 6.0% for 200 μM SP$_{30}\beta$ and 33.7 ± 5.1% for 200 μM SP$_{30}\gamma$). However, the inhibitory effect of these peptides on $\alpha\beta_{\Delta C}\gamma_{\Delta C}$-rENaC was more than additive in a 1:1 (100 μM total SP concentration) $\beta + \gamma$ mixture (69.4 ± 7.2%; bottom trace). This observation is consistent with an interaction between the β and γ peptides and is in concordance with the intrinsic tyrosine fluorescence measurements presented earlier (Figure 2).

The degree of peptide inhibition was compared at different concentrations of the individual SP$_{30}\beta$ and SP$_{30}\gamma$ peptides alone and in a 1:1 mixture for channels composed of WT α-rENaC and $\beta_{\Delta C}$ and $\gamma_{\Delta C}$-rENaC (Figure 5). The inhibitory effect of both SP$_{30}\beta$ (Figure 5A) and SP$_{30}\gamma$ (data not shown) on basal-activated ENaC was concentration dependent. Second, open, and closed time histogram analyses of these data revealed that these peptides induced the appearance of a second closed state (as compared to the single closed state of $\alpha\beta_{\Delta C}\gamma_{\Delta C}$-rENaC; top trace). Channel mean open time (τ_o) or the meantime of the first closed state (τ'_c) was not affected by these peptides.

If the hypothesis that the carboxy-terminal regions of the β- and γ-ENaC subunits act as channel-gating particles is correct, exogenous β- and γ-hENaC peptides individually or in combination should not block wild-type $\alpha\beta\gamma$-rENaC because of the presence of the intrinsic carboxy terminal β and γ subunit regions within the functional channel complex. This prediction was tested, and the results are shown in Figure 6. Neither the individual peptides nor a combination of 100 μM SP$_{30}\beta$ plus 100 μM SP$_{30}\gamma$ produced any effect on the WT $\alpha\beta\gamma$-rENaC. Dwell time histogram analysis of these single channel data indicated that the time spent by wild-type $\alpha\beta\gamma$-rENaC in its closed state was distributed as a double exponential ($\tau'_c = 21 \pm 6$ ms, and $\tau''_c = 260 \pm 39$ ms). The open time histograms of $\alpha\beta\gamma$-rENaC could be fit to a single exponential ($t_o = 140 \pm 35$ ms). These values were not affected by the addition of either one of the individual peptides or their mixture.

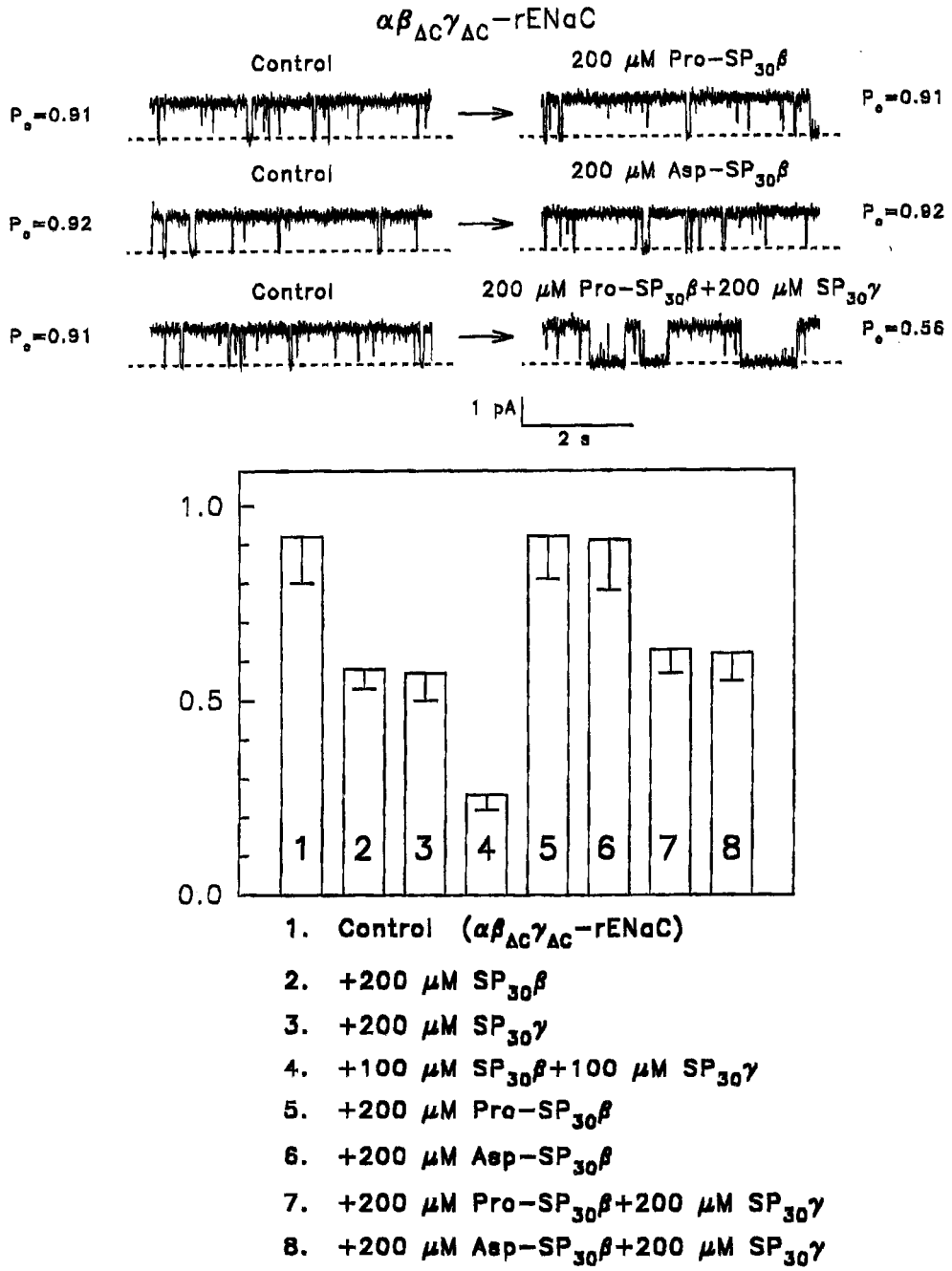

FIGURE 7: Effect of Pro- and Asp-substituted C-terminal β peptides (Pro-$SP_{30}\beta$ and Asp-$SP_{30}\beta$) individually or in combination with the authentic γ peptide on $\alpha\beta_{\Delta C}\gamma_{\Delta C}$-rENaC activity in planar bilayers. (A) Single channel recordings. Conditions were the same as in Figure 3. Each experiment was repeated at least four times, with similar results. (B) Bar graph summary.

We next performed experiments to test the hypothesis that the synergy of inhibition produced by the simultaneous presence of both the β- and γ-hENaC C-terminal peptides resulted from β-sheet formation between the two peptides. We designed peptides corresponding to the (β-hENaC) C-terminal sequence in which the strong β-sheet forming amino acids isoleucine (I) and valine (V) were substituted by either proline (P) or aspartic acid (D), both β-sheet breaking amino acids. In single channel experiments, these substituted β-hENaC peptides were unable to inhibit basal-activated Na^+ channels (Figure 7). Moreover, combinations of either substituted β-hENaC peptides (Pro-$SP_{30}\beta$ or Asp-$SP_{30}\beta$) with wild-type $SP_{30}\gamma$ peptide resulted in an inhibition essentially identical to the individual $SP_{30}\gamma$ curve. In addition, the decrease in tyrosine fluorescence quantum yield was less in mixtures of these substituted β-hENaC peptides with wild-type $SP_{30}\gamma$ peptide, as compared to mixtures with wild-type $SP_{30}\beta$- and $SP_{30}\gamma$ peptides (Table 1). Plotting $1/\tau_c''$ (τ_c'' is the mean closed time of the second closed state) versus peptide concentration (Figure 8) indicated that the major effect of these peptides was to "lock" the channel in a second closed state (now resembling the wild-type channel) and that there was a synergy between the β- and γ-peptides in producing this effect.

DISCUSSION

The defining characteristic of Liddle's hypertension is the basal-activation of an amiloride-sensitive sodium channel, ENaC. Expression of the Liddle's phenotype has been linked to mutations in the C-terminal cytoplasmic tail of the β

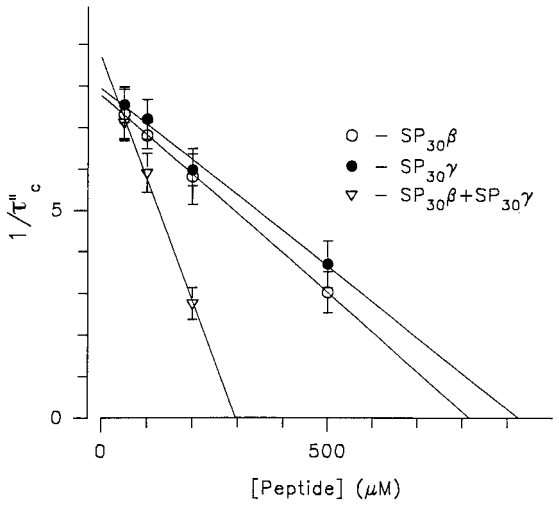

FIGURE 8: Reciprocal plot ($1/\tau''_c$) of the second closed state dwell time (τ''_c) versus β or γ and β and γ blocking peptide concentration. Data points represent mean values ± 1 SD for four experiments. Control peptides (a 14-mer identical to the last amino acids of CFTR and a random 26-mer peptide were without effect, not shown).

subunit of ENaC, although mutations in the C-terminal of the γ subunit also give rise to a Liddle's-like hypertensive state *(7, 8, 13, 14, 35−39)*. The originally identified mutation (insertion of a premature stop codon at arginine 564) produces an increased macroscopic Na^+ current in heterologous expression systems. This increased macroscopic amiloride-sensitive Na^+ current has been postulated to result from an altered ENaC with an increased open probability and/or the presence of more channels at the cell's surface. Another hypothesis suggests that mutations in ENaC producing Liddle's disease inhibit feedback inhibition of the channel by intracellular Na^+ (*40*). Other β subunit mutations resulting in C-terminal truncations also lead to a hypertensive phenotype, as do several recently identified point mutations in the C-terminus (P616L and W594H; see refs *35* and *39*).

We have previously observed that synthetic peptides comprising the last 10 amino acids of either β-, γ-hENaC, β-rENaC, or the last 30 amino acids of β-hENaC, can inhibit the basal-activated Na^+ channel immunopurified from the lymphocytes of Liddle's patients (*18, 34*). Examination of the peptide sequences of the β- and γ-blocking peptides reveals that these peptides contain several negatively charged residues interspersed by neutral hydrophobic amino acids. In contrast, synthetic peptides that contained negative residues in a different sequence or where the negative residues were changed to neutral glycines were ineffective as blockers of ENaC. Moreover, the terminal 10 or 30 residues of α-hENaC did not block the channel. Thus, the C-terminal tail of both β- and γ-hENaC subunits may act as intrinsic gating particles of ENaC, reminiscent of the behavior of the 20 amino acid region at the NH_2 terminal of voltage-activated K^+ channels (*21, 22, 41, 42*).

In this regard, the ball-and-chain model proposed for K^+ channel gating views the NH_2-terminal as an open channel blocker, i.e., the last 20 amino acids act as a "cork", occluding the pore. An alternative mechanism is one in which the binding site is distinct from the pore proper and inhibition occurs via conformational changes of the channel superstructure due to allosteric effects of the antagonist (*43*). The distinction between these mechanisms can be made on the basis of kinetic analyses at different concentrations of antagonist (*41, 42*). The case of ENaC with two antagonists (β- and γ-peptide) may even be more complex in that both peptides may be binding to the same site (within or outside the pore itself) or, alternatively, one peptide (either β or γ) may act via occlusion of the conduction pathway while the other may interact at a different site, perhaps increasing the efficiency of the inhibition. If either of the peptides separately or in combination were occluding the pore, then the inhibition would appear as a dose-dependent decrease of the channel open or burst time, assuming the blockade was slower than the gating kinetics (*41, 42*). In contrast to these predictions, analyses of the open and closed time histograms constructed from recordings of these channels in the presence of increasing peptide concentrations demonstrated that the decrease in open probability in the presence of $SP_{30}\beta$ or $SP_{30}\gamma$ separately or together was due to changes in distribution of time spent by the channel in the closed, but not in the open state. At all concentrations examined, addition of the peptides resulted in a second slow component in the distribution of the channel closed time (τ''), in contrast to the single exponentially distributed closed time of $\alpha\beta_{\Delta C}\gamma_{\Delta C}$-rENaC in the absence of peptides. Importantly, the peptides did not affect the duration of channel mean open time (τ_o) or the burst time (τ_{burst}, data not shown). The faster component of the channel closures (τ'_c) also remained constant at all peptide concentrations. Thus, the peptides do not act as open channel blockers; the major effect of these inhibitory peptides was to "lock" the channel in a closed state. On the basis of these findings, we conclude that the gating mechanism of $\alpha\beta\gamma$-ENaC is rather different from the "ball-and-chain" mechanism that served as a prototype for these studies.

The present experiments extend our initial observations, directly testing the hypothesis that truncated β- or γ-rENaC, combined with wild-type α-rENaC in planar lipid bilayers, produces a basal-activated channel. Moreover, we found that peptides comprised of the last 30 amino acids of either the β- or γ-hENaC subunit can inhibit this basal-activated channel. As indicated above, the last 10 amino acids within the sequence of the synthetic peptides contain 3 or 4 negatively charged amino acids (aspartic or glutamic acid). Although replacement of negatively charged residues in these short blocking peptides produced a noninhibitory peptide, it may not be only the charges themselves that are important, but also the ability that these peptides have to form a β-sheet structure. As a mature ENaC requires the expression of an $\alpha\beta\gamma$ subunit complex and as only the β- or γ-ENaC C-termini can form a β-sheet structure and act as inhibitory peptides, we tested the hypothesis that the putative gating particle could be comprised of a two-strand, antiparallel β sheet, each half of which would be contributed by the C-terminal tail of the β and γ subunit. In partial support of this hypothesis, we found that the effects of adding the C-terminal β- and γ-hENaC 30 amino acid residue peptides together to the basal-activated ENaC channel incorporated into a planar lipid bilayer produced a greater-than-additive inhibition of the channel than either peptide alone. These peptides could not inhibit Na^+ channels comprised of wild-type $\alpha\beta\gamma$-rENaC, channels in which the carboxy terminal β- and γ-tails are present. In further support of this idea, the amino acids isoleucine and valine were replaced by the

β-sheet breaking amino acids proline or aspartic acid, and these substitutions resulted in peptides that were unable to affect basal-activated ENaC.

Although our results strongly suggest that the C-terminal region of the β- and γ-ENaC subunits act as intrinsic gating particles, these results do not speak to the issue of whether a trafficking event (i.e., increased cell surface delivery or decreased rate of channel endocytosis) is also involved in the increased macroscopic currents seen in heterologous expression systems. In fact, recent work of several groups suggests that the WW binding domain-rich intracellular protein Nedd4, which also contains a ubiquitin ligase domain, binds specifically to a proline-rich region in the C-terminus of both the β- and γ-ENaC subunits. Absence of this region has been shown to greatly affect surface expression of this channel (*15*, *17*, *38*, *44*). Thus, we propose that both mechanisms, namely, an increase in P_o and an increase in channel surface expression, may be operative, and different mutations, e.g., truncation versus point mutations, may result in a predominance of one mechanism over the other. However, very few single channel measurements have been made on channels containing these mutations to either confirm or refute this hypothesis.

Because the α subunit forms the conduction region of ENaC (see refs *28* and *45* and Figure 3), the manner in which the C-terminal tails of β- and γ-ENaC interact with the inner mouth region of the pore in the conductive α subunit of ENaC will yield insights into the regulation of channel gating, precisely that property of channel behavior that at least in part is responsible for Liddle's hypertension. Because α-ENaC itself can form a functional Na^+ channel, there must be a yet unknown intrinsic gating mechanism in α-ENaC alone. It has been hypothesized that the N-terminus of the α-subunit may be important in this regard (*38*). Because the overall gating properties of α-ENaC versus $\alpha\beta\gamma$-ENaC do not differ (see Figure 3) and because the elimination of the cytoplasmic C-terminal tails of either or both of the β- and γ-ENaC subunits substantially increase single channel P_o (Figure 4), there must be at least two separate gating processes: one inherent to α-ENaC alone and one imposed onto the complex by the β- and γ-ENaC C-terminal tails. The results presented here support such a paradigm.

ACKNOWLEDGMENT

We thank Cathleen Guy for outstanding assistance in the preparation of this manuscript.

REFERENCES

1. Warnock, D. G., and Bubien, J. K. (1995) *Am. J. Kidney Dis. 25*, 924−927.
2. Warnock, D. G., and Bubien, J. K. (1994) *Hosp. Pract. 29*, 95−105.
3. Lifton, R. P. (1996) *Science 272*, 676−680.
4. Liddle, G. W., Bledsoe, T., and Coppage, W. S. (1963) *Trans. Am. Assoc. Phys. 76*, 199−213.
5. Botero-Velez, M., Curtis, J. J., and Warnock, D. G. (1994) *N. Engl. J. Med. 330*, 178−181.
6. Gadallah, M. F., Abreo, K., and Work, J. (1995) *Am. J. Kidney Dis.* 25, 924−927.
7. Shimkets, R. A., Warnock, D. G., Bositis, C. M., Nelson-Williams, C., Hansson, J. H., Schambelan, M., Gill, J. R. J., Ulick, S., Milora, R. V., Findling, J. W., Canessa, C. M., Rossier, B. C., and Lifton, R. P. (1994) *Cell 79*, 407−414.
8. Hansson, J. H., Nelson-Williams, C., Suzuki, H., Schild, L., Shimkets, R., Lu, Y., Canessa, C., Iwasaki, T., Rossier, B., and Lifton R. (1995a) *Nature Genet.* 11, 76−82.
9. Warnock, D. G. (1996) *J. Am. Soc. Nephrol. 7*, 2490−2494.
10. Rossier, B. C. (1997) *J. Am. Soc. Nephrol. 8*, 980−992.
11. Warnock, D. G. (1998) *Kidney Int. 53*, 18−24.
12. Schild, L., Canessa, C. M., Shimkets, R. A., Gautschi, I., Lifton, R. P., and Rossier, B. C. (1995) *Proc. Natl. Acad. Sci. U.S.A. 92*, 5699−5703.
13. Snyder, P. M., Price, M. P., McDonald, F. J., Adams, C. M., Volk, K. A., Zelher, B. G., Stokes, J. B., and Welsh, M. J. (1996) *Cell 83*, 969−978.
14. Tamura, H., Schild, L., Enomoto, N., Matsui, N., Marumo, F., Rossier, B. C., and Sasaki, S. (1996) *J. Clin. Invest. 97*, 1780−1784.
15. Staub, O., Dho, S., Henry, P. C., Correa, J., Ishikawa, T., McGlade, J., and Rotin, D. (1996) *EMBO J. 15*, 2371−2380.
16. Shimkets, R. A., Lifton, R. P., and Canessa, C. M. (1997) *J. Biol. Chem. 272*, 25537−25541.
17. Staub, O., Yeger, H., Plant, P. J., Kim, H., Ernst, S. A., and Rotin D. (1997) *Am. J. Physiol. 272*, C1871−C1880.
18. Ismailov, I. I., Berdiev, B. K., Fuller, C. M., Bradford, A. L., Lifton, R. P., Warnock, D. G., Bubien, J. K., and Benos, D. J. (1996) *Am. J. Physiol. 270*, C214−C223.
19. Firsov, D., Schild, L., Gautschi, I., Merillat, A. M., Schneeberger, E., and Rossier, B. C. (1996) *Proc. Natl. Acad. Sci. U.S.A. 93*, 15370−15375.
20. Awayda, M. S., Tousson, A., and Benos, D. J. (1997) *Am. J. Physiol. 273*, C1889−C1899.
21. Hoshi, T. Zagotta, W. N., and Aldrich, R. W. (1990) *Science 250*, 533−538.
22. Zagotta, W. N., Hoshi, T., and Aldrich, R. W. (1990) *Science 250*, 568−571.
23. Woody, R. W. (1985) in *The Peptides*, (Hruby, V. J., Ed.) Vol. 7, pp 15−114, Academic Press, New York.
24. Chang, C. T., Wu, C.-S. C., and Yang, J. T. (1973) *Anal. Biochem. 91*, 13−31.
25. Chen, R. F. (1967) in *Fluorescence. Theory, Instrumentation, and Practice* (Guilbault, G. G., Ed.) pp 443−509, Marcel Dekker, Inc., New York.
26. Giacoutti, V., Fouda M., and Crane-Robinson, C. (1977) *Biophys. Chem. 6*, 379−383.
27. Winder, A. F., and Gent, W. L. G. (1971) *Biopolymers 10*, 1243−1251.
28. Berdiev, B. K., Prat, A. G., Cantiello, H. F., Ausiello, D. A., Fuller, C. M., Jovov, B., Benos, D. J., and Ismailov, I. I. (1996) *J. Biol. Chem. 273*, 17704−17710.
29. Ismailov, I. I., Awayda, M. S., Berdiev, B. K., Bubien, J. K., Lucas, J. E., Fuller, C. M., and Benos, D. J. (1996) *J. Biol. Chem. 271* (2), 807−816.
30. Ismailov, I. I., Shlyonsky, V.-Gh., and Benos, D. J. (1997) *Proc. Natl. Acad. Sci. U.S.A. 94*, 7651−7654.
31. Berdiev, B. K., Karlson, K. H., Jovov, B., Ripoll, P.-J., Morris, R., Loffing-Cueni, D., Halpin, P., Stanton, B. A., Kleyman, T. R., and Ismailov, I. I. (1998) *Biophys. J. 75*, 2292−2301.
32. Manning, M. C. and Woody, R. W. (1987) *Biopolymers 26*, 1731−1752.
33. Wu, J., Yang, J. T., and Wu, C.-S. C. (1992) *Anal. Biochem. 200*, 359−364.
34. Bubien, J. K., Ismailov, I. I., Berdiev, B. K., Cornwell, T., Lifton, R. P., Fuller, C. M., Achard, J. M., Benos, D. J., and Warnock, D. G. (1996) *Am. J. Physiol. 270*, C208−C213.
35. Hansson, J. H., Schild, L., Lu, Y., Wilson, T. A., Gautschi, I., Shimkets, R., Nelson-Williams, C., Rossier, B., and Lifton, R. (1995b) *Proc. Natl. Acad. Sci. U.S.A. 92*, 11495−11499.
36. Jeunemaitre, X., Bassilana, F., Persu, A., Dumont, C., Champigny, G., Lazdunski, M., Corvol, P., and Barbry, P. (1997) *J. Hypertens. 15*, 1091−1100.
37. Oh, Y., and Warnock, D. G. (1997) *J. Am. Soc. Nephrol. 8*, 126−129.
38. Schild, L., Lu, Y., Gautschi, I., Schneeberger, E., Lifton, R. P., and Rossier, B. C. (1996) *EMBO J. 15*, 2381−2387.

39. Su, Y. R., Rutkowski, M. P., Klanke, C. A., Wu, X., Cui, Y., Pun, R. Y. K., Carter, V., Reif, M., and Menon, A. G. (1996) *J. Am. Soc. Neph. 7*, 2543−2549.
40. Kellenberger, S., Gautschi, I., Rossier, B. C., and Schild, L. (1998) *J. Clin. Invest. 101* (12), 2741−2750.
41. Toro, L., Stefani, E., and Latorre, R. (1992) *Neuron 9*, 237−245.
42. Toro, L., Ottolia, M., Stefani, E., and Latorre, R. (1994) *Biochemistry 33*, 7220−7228.
43. Hille, B. (1992) *Ionic Channels of Excitable Membranes*, 2nd ed., Sinauer Assoc. Inc., Sunderland, MA.
44. Rotin, D., Bar-Sagi, D., O'Brodovich, H., Merlainen, J., Lehto, V. P., Caness, C. M., Rossier, B. C., and Downey, G. P. (1994) *EMBO J. 13*, 4440−4450.
45. Canessa, C. M., Horisberger, J. D., and Rossier, B. C. (1993) *Nature 361*, 467−470.

BI981979S